



Michael Leighton Beaman
Stefan Bader

:author

Assistant Professor of Architecture, University of Texas, Austin
'Dipl. Ing. Arch.' candidate, Technical University of Munich
United States
Germany

:organization

:country

Responsive Shading | Intelligent Façade Systems

As issues of sustainability gain traction for architects, methodologies for designing, analyzing, and calibrating design solutions have emerged as essential areas of research and development. A number of approaches have been pursued with regard to embedding data into the design process, most fall into one of two approaches to research. The first approach is to mediate environmental impact at the level of applied technology; the second alters building methods and material construction, generating efficient energy use. However, few approaches deal with the crafting of relationships between information and performance on an architectural level. We will examine an approach focused on understanding how crafting relationships between information and design can move architecture towards achieving sustainability.

:abstract

In developing this approach, we created a data-driven design methodology spanning from design inception to construction. Data-driven models, common in the fields of natural science, offer a method to generate and test a multiplicity of responsive solutions. By contextualizing the solutions generated, we were able design through a set of specific and controlled responses rather than as a singular solution. Information utilization requires a new kind of craft that moves beyond instances into relationships and offers performance sensitive issues in design a focused trajectory.

We applied this method to the research and development of a responsive shading structure built in conjunction with a thermal testing lab for two test locations – Austin, Texas (Figure. 1 and 2) and Munich, Germany. The following paper chronicles the design and construction at the Texas site over an academic semester.



1 Sustainability as Design Context

As issues of sustainability gain traction for architects, methodologies for designing, analyzing, and calibrating design solutions have emerged as essential areas of research and development. A number of approaches have been pursued with regard to embedding data into the design process, most fall into one of two approaches to research. The first approach is to mediate environmental impact at the level of applied technology; the second approach is to alter building methods and material construction generating efficient energy use. However, few approaches deal with the crafting of relationships between information and performance on an architectural level. This paper will examine a design approach focused on understanding how crafting relationships between information and design can move architecture towards achieving sustainability.

In order to better understand how relationships between information and design can move architecture towards achieving sustainability, we proposed creating a data-driven methodology that spans from design inception through to construction. In this paper, we will examine the process developed in designing for a responsive shading structure over the course of an academic semester. Using both conventional and advanced analytical and generative techniques, we developed a relational model that produced solution families within a strict parameter set. With the our requirement of sustainability to be performance driven, we calibrated our process to achieve optimized results for a number of metrics.

2 Responsive Solar Shading Façade | Goals and Methods

The solar shading structure was initially developed with a data-driven design methodology to incorporate meaningful information as a transformative device. We first began by constructing a responsive parametric model generated from contextual, phenomenological, and solar data. Our test case utilized this model to generate a structurally rigid shading system that provided better shading performance than generically generated shading configurations (1). We focused our digital model on creating effective day-long shading during high thermal gain seasons and planar with any façade surface we choose to apply at any global location. The data collected had to impact the parametric model

with specificity, in order to define a number of design criteria as quantitative and geometric definitions. We also limited the paths through which input data created outputs allowing us to focus on designing a shading system composed of self-similar components. The shape of the component is determined by specific solar data for any given site, volumetric context, and climatologically conditions; the component size and accumulation pattern is determined by a number of phenomenological conditions. The combination led to a data-driven parametric model that was used to test a variety of configurations and simulate performance results. The parametric model also allowed us to refine the articulation of our shading strategy into a family of solutions that meet specified criteria.

The site for generating and testing our shading structure is a newly completed thermal lab located in Austin, Texas. The thermal lab is a thermally broken and highly insulated building equipped to record solar radiation, temperature, light levels, heat gain, and humidity within its singular space, in addition to basic meteorological data exterior to the building's environment (Figure 3 and 6). The lab has a single glazed south facing façade measuring twelve feet by nine feet and is approximately 22 feet above grade. The solar shading façade we designed, constructed and tested was the first use of this new facility.

3 Data-Driven Analysis

As a starting point to the design process, we required two sets of comparative analytical data—solar norms and an analysis of shading strategies. Solar norms are the three-dimensional sun path for our given test site, surface exposure relative to our test façade, a base reading of solar radiation, light levels from our site and orientation, and local obstructions and view corridors. The information collected from these variables, fall into two categories of data—geometric and numerical. Given the difference in usable data, we needed a methodology for combining and instrumentalizing this information. We began by composing a parametric sun-path generator that also calculated the exposure plane of any set of input surfaces within its volumetric context. Using Grasshopper + Rhinoceros and a small set of custom VB scripts, we were able to construct a parametric definition that produced calculations for areas of exposure with a specific set of output data. We later utilized this data to generate the three-dimensional shading structure and



Figure 1. Shading structure in place on Thermal Lab



Figure 2. Shading structure detail in place on Thermal Lab

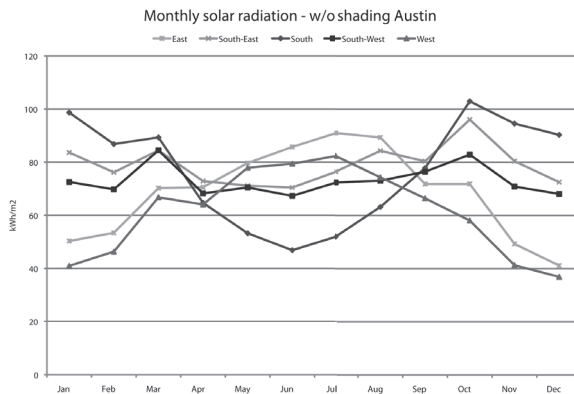


Figure 3. Solar radiation for site 1 - Austin , Texas

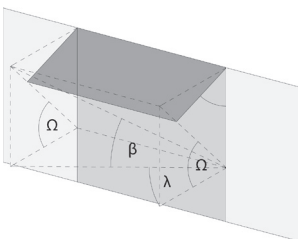


Figure 4. Horizontal shading device geometric model

simulate their performance with Eco-tech before final construction. Radiation data; however, needed real world data collection. Over a number of weeks, we collected solar radiation levels in our thermal lab (Figure 3 and 5). We coordinated the real world data with our parametric model and combined these with conventional shading calculations to construct the second set of information— an analysis of conventional shading strategies.

The information for conventional shading devices was simulated using our modified parametric model. Conventional shading devices by our definition were horizontal or vertical louver systems or orthogonal grid structures (Figure 4 and 5). To determine shading devices to test, we created a set of configurations based on prototypical "shadow-line angle" methods. In (Figure 4 and 5):

- $\tan W = \tan b / \tan g$
- where W = profile or shadow-line angle
- b = solar altitude angle
- g = solar azimuth angle

These shading devices can be calibrated by rotation and scale in length and width. Because their effect is generated from two-dimensional surfaces, these devices have difficulty remaining effective throughout the total solar arc. Figure 4 explains how to use the shadow-line angle to tilt the horizontal shading device to provide maximum shading. This angle represents maximum shading for a specific position of the sun. To receive maximum shading over a specific duration, this angle has to be changed respectively. An example has been created for Austin, Texas on March / September (Figure 7).

- $c = W$
- where c = angle for tilting of horizontal shading device to provide maximum shading

We discovered with vertical shading structures, maximum shading with a minimum structure is achieved when the azimuth angle of the sun is perpendicular to the surface of the shading structure. Also, the smaller the shading surface, the lower the effective shading and the tighter the spacing of components must be to compensate. In addition, the vertical surfaces need to rotate throughout the day respectively to the azimuth angle g of the sun to continue to be effective day-long (Figure 7).

- $w = g$
- where w = angle for rotating of vertical shading device to provide maximum shading
- g = solar azimuth angle

Neither horizontal nor vertical devices are effective throughout the entire day, and no single configuration is effective at a variety of orientations. Typically, horizontal devices are effective on southern facades for high solar paths, but are unable to block low sun vectors. Vertical surfaces are effective for east and west facades, but only at moderate to low sun angles. Grid configurations, a combination of horizontal and vertical surfaces have been developed as more effective shading solutions (Figure 8). We tested these creating prototypical surface configurations based on excepted technical standards and simulating the amount of solar penetration. A comparative analysis can be seen in Figure 15.

For our Austin, Texas site, these orthogonal or rotated geometries are most effective in south, southwest, and west orientations, respectively. However, due to its accumulation of two-dimensional surfaces, it suffers similar limitations of vertical and horizontal surfaces. Our study showed that with a greater width to height ratio, there would be a greater effective per linear foot of exposed surface. Extruding the surfaces further than conventional formulas recommend does increase effectiveness at lower sun angles, but greatly reduces visibility. Surface rotation allowing for the calibration worked well, but adds a level of complexity to any shading configuration by requiring two separate degrees of freedom. In this case, a secondary support structure as well as mechanisms to allow for this range of motion would be necessary. Though we could clearly see the limitations of conventional systems, this analysis provided us with insight into how we might begin to configure our test structure as well as begin to define base geometric definitions.

4 Data-driven Parameters

Based on our analysis of conventional shading structures, we chose a grid configuration developed with a three-dimensional articulation based on a variety of data sets. We began by developing the three-dimensional relationships between the path of the sun at any given position and its subsequent shadow surface. From this information, we developed each shading component

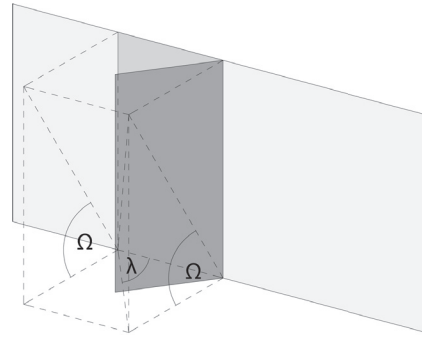


Figure 5. Vertical shading device geometric model

A Sample of simulated horizontal shading structure

Year	Jan	Feb	Mar	Apr	May	Jun	Jul	Aug	Sept	Oct	Nov	Dec
2001-2002	14.2	17.2	14.8	14.8	11.8	11.3	10.1	10.7	11.6	14.5	15.5	15.1
2002-2003	9	10.9	10	10.4	10.4	10.8	11.8	12.1	12.1	12.1	12.4	12.4
2003-2004	8.8	10.8	10.8	10.8	10.8	11.3	11.3	11.3	11.3	11.3	11.3	11.3
2004-2005	8.7	10.7	10.7	10.7	10.7	11.2	11.2	11.2	11.2	11.2	11.2	11.2
2005-2006	8.7	10.7	10.7	10.7	10.7	11.2	11.2	11.2	11.2	11.2	11.2	11.2
2006-2007	8.7	10.7	10.7	10.7	10.7	11.2	11.2	11.2	11.2	11.2	11.2	11.2
2007-2008	8.7	10.7	10.7	10.7	10.7	11.2	11.2	11.2	11.2	11.2	11.2	11.2
2008-2009	8.7	10.7	10.7	10.7	10.7	11.2	11.2	11.2	11.2	11.2	11.2	11.2
2009-2010	8.7	10.7	10.7	10.7	10.7	11.2	11.2	11.2	11.2	11.2	11.2	11.2
2010-2011	8.7	10.7	10.7	10.7	10.7	11.2	11.2	11.2	11.2	11.2	11.2	11.2
2011-2012	8.7	10.7	10.7	10.7	10.7	11.2	11.2	11.2	11.2	11.2	11.2	11.2
2012-2013	8.7	10.7	10.7	10.7	10.7	11.2	11.2	11.2	11.2	11.2	11.2	11.2
2013-2014	8.7	10.7	10.7	10.7	10.7	11.2	11.2	11.2	11.2	11.2	11.2	11.2
2014-2015	8.7	10.7	10.7	10.7	10.7	11.2	11.2	11.2	11.2	11.2	11.2	11.2
2015-2016	8.7	10.7	10.7	10.7	10.7	11.2	11.2	11.2	11.2	11.2	11.2	11.2
2016-2017	8.7	10.7	10.7	10.7	10.7	11.2	11.2	11.2	11.2	11.2	11.2	11.2
2017-2018	8.7	10.7	10.7	10.7	10.7	11.2	11.2	11.2	11.2	11.2	11.2	11.2
2018-2019	8.7	10.7	10.7	10.7	10.7	11.2	11.2	11.2	11.2	11.2	11.2	11.2
2019-2020	8.7	10.7	10.7	10.7	10.7	11.2	11.2	11.2	11.2	11.2	11.2	11.2
2020-2021	8.7	10.7	10.7	10.7	10.7	11.2	11.2	11.2	11.2	11.2	11.2	11.2
2021-2022	8.7	10.7	10.7	10.7	10.7	11.2	11.2	11.2	11.2	11.2	11.2	11.2
2022-2023	8.7	10.7	10.7	10.7	10.7	11.2	11.2	11.2	11.2	11.2	11.2	11.2
2023-2024	8.7	10.7	10.7	10.7	10.7	11.2	11.2	11.2	11.2	11.2	11.2	11.2
2024-2025	8.7	10.7	10.7	10.7	10.7	11.2	11.2	11.2	11.2	11.2	11.2	11.2
2025-2026	8.7	10.7	10.7	10.7	10.7	11.2	11.2	11.2	11.2	11.2	11.2	11.2
2026-2027	8.7	10.7	10.7	10.7	10.7	11.2	11.2	11.2	11.2	11.2	11.2	11.2
2027-2028	8.7	10.7	10.7	10.7	10.7	11.2	11.2	11.2	11.2	11.2	11.2	11.2
2028-2029	8.7	10.7	10.7	10.7	10.7	11.2	11.2	11.2	11.2	11.2	11.2	11.2
2029-2030	8.7	10.7	10.7	10.7	10.7	11.2	11.2	11.2	11.2	11.2	11.2	11.2
2030-2031	8.7	10.7	10.7	10.7	10.7	11.2	11.2	11.2	11.2	11.2	11.2	11.2
2031-2032	8.7	10.7	10.7	10.7	10.7	11.2	11.2	11.2	11.2	11.2	11.2	11.2
2032-2033	8.7	10.7	10.7	10.7	10.7	11.2	11.2	11.2	11.2	11.2	11.2	11.2
2033-2034	8.7	10.7	10.7	10.7	10.7	11.2	11.2	11.2	11.2	11.2	11.2	11.2
2034-2035	8.7	10.7	10.7	10.7	10.7	11.2	11.2	11.2	11.2	11.2	11.2	11.2
2035-2036	8.7	10.7	10.7	10.7	10.7	11.2	11.2	11.2	11.2	11.2	11.2	11.2
2036-2037	8.7	10.7	10.7	10.7	10.7	11.2	11.2	11.2	11.2	11.2	11.2	11.2
2037-2038	8.7	10.7	10.7	10.7	10.7	11.2	11.2	11.2	11.2	11.2	11.2	11.2
2038-2039	8.7	10.7	10.7	10.7	10.7	11.2	11.2	11.2	11.2	11.2	11.2	11.2
2039-2040	8.7	10.7	10.7	10.7	10.7	11.2	11.2	11.2	11.2	11.2	11.2	11.2
2040-2041	8.7	10.7	10.7	10.7	10.7	11.2	11.2	11.2	11.2	11.2	11.2	11.2
2041-2042	8.7	10.7	10.7	10.7	10.7	11.2	11.2	11.2	11.2	11.2	11.2	11.2
2042-2043	8.7	10.7	10.7	10.7	10.7	11.2	11.2	11.2	11.2	11.2	11.2	11.2
2043-2044	8.7	10.7	10.7	10.7	10.7	11.2	11.2	11.2	11.2	11.2	11.2	11.2
2044-2045	8.7	10.7	10.7	10.7	10.7	11.2	11.2	11.2	11.2	11.2	11.2	11.2
2045-2046	8.7	10.7	10.7	10.7	10.7	11.2	11.2	11.2	11.2	11.2	11.2	11.2
2046-2047	8.7	10.7	10.7	10.7	10.7	11.2	11.2	11.2	11.2	11.2	11.2	11.2
2047-2048	8.7	10.7	10.7	10.7	10.7	11.2	11.2	11.2	11.2	11.2	11.2	11.2
2048-2049	8.7	10.7	10.7	10.7	10.7	11.2	11.2	11.2	11.2	11.2	11.2	11.2
2049-2050	8.7	10.7	10.7	10.7	10.7	11.2	11.2	11.2	11.2	11.2	11.2	11.2
2050-2051	8.7	10.7	10.7	10.7	10.7	11.2	11.2	11.2	11.2	11.2	11.2	11.2
2051-2052	8.7	10.7	10.7	10.7	10.7	11.2	11.2	11.2	11.2	11.2	11.2	11.2
2052-2053	8.7	10.7	10.7	10.7	10.7	11.2	11.2	11.2	11.2	11.2	11.2	11.2
2053-2054	8.7	10.7	10.7	10.7	10.7	11.2	11.2	11.2	11.2	11.2	11.2	11.2
2054-2055	8.7	10.7	10.7	10.7	10.7	11.2	11.2	11.2	11.2	11.2	11.2	11.2
2055-2056	8.7	10.7	10.7	10.7	10.7	11.2	11.2	11.2	11.2	11.2	11.2	11.2
2056-2057	8.7	10.7	10.7	10.7	10.7	11.2	11.2	11.2	11.2	11.2	11.2	11.2
2057-2058	8.7	10.7	10.7	10.7	10.7	11.2	11.2	11.2	11.2	11.2	11.2	11.2
2058-2059	8.7	10.7	10.7	10.7	10.7	11.2	11.2	11.2	11.2	11.2	11.2	11.2
2059-2060	8.7	10.7	10.7	10.7	10.7	11.2	11.2	11.2	11.2	11.2	11.2	11.2
2060-2061	8.7	10.7	10.7	10.7	10.7	11.2	11.2	11.2	11.2	11.2	11.2	11.2
2061-2062	8.7	10.7	10.7	10.7	10.7	11.2	11.2	11.2	11.2	11.2	11.2	11.2
2062-2063	8.7	10.7	10.7	10.7	10.7	11.2	11.2	11.2	11.2	11.2	11.2	11.2
2063-2064	8.7	10.7	10.7	10.7	10.7	11.2	11.2	11.2	11.2	11.2	11.2	11.2
2064-2065	8.7	10.7	10.7	10.7	10.7	11.2	11.2	11.2	11.2	11.2	11.2	11.2
2065-2066	8.7	10.7	10.7	10.7	10.7	11.2	11.2	11.2	11.2	11.2	11.2	11.2
2066-2067	8.7	10.7	10.7	10.7	10.7	11.2	11.2	11.2	11.2	11.2	11.2	11.2
2067-2068	8.7	10.7	10.7	10.7	10.7	11.2	11.2	11.2	11.2	11.2	11.2	11.2
2068-2069	8.7	10.7	10.7	10.7	10.7	11.2	11.2	11.2	11.2	11.2	11.2	11.2
2069-2070	8.7	10.7	10.7	10.7	10.7	11.2	11.2	11.2	11.2	11.2	11.2	11.2
2070-2071	8.7	10.7	10.7	10.7	10.7	11.2	11.2	11.2	11.2	11.2	11.2	11.2
2071-2072	8.7	10.7	10.7	10.7	10.7	11.2	11.2	11.2	11.2	11.2	11.2	11.2
2072-2073	8.7	10.7	10.7	10.7	10.7	11.2	11.2	11.2	11.2	11.2	11.2	11.2
2073-2074	8.7	10.7	10.7	10.7	10.7	11.2	11.2	11.2	11.2	11.2	11.2	11.2
2074-2075	8.7	10.7	10.7	10.7	10.7	11.2	11.2	11.2	11.2	11.2	11.2	11.2
2075-2076	8.7	10.7	10.7	10.7	10.7	11.2	11.2	11.2	11.2	11.2	11.2	11.2
2076-2077	8.7	10.7	10.7	10.7	10.7	11.2	11.2	11.2	11.2	11.2	11.2	11.2
2077-2078	8.7	10.7	10.7	10.7	10.7	11.2	11.2	11.2	11.2	11.2	11.2	11.2
2078-2079	8.7	10.7	10.7	10.7	10.7	11.2	11.2	11.2	11.2	11.2	11.2	11.2
2079-2080	8.7	10.7	10.7	10.7	10.7	11.2	11.2	11.2	11.2	11.2	11.2	11.2
2080-2081	8.7	10.7	10.7	10.7	10.7	11.2	11.2	11.2	11.2	11.2	11.2	11.2
2081-2082	8.7	10.7	10.7	10.7	10.7	11.2	11.2					

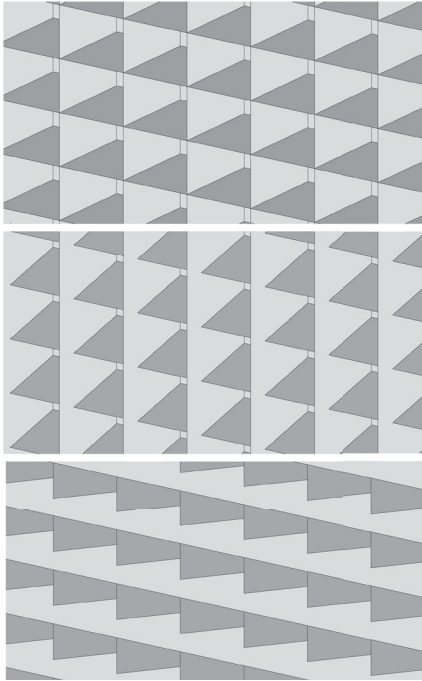


Figure 8. Grid shading devices (vertical + horizontal surface accumulation)

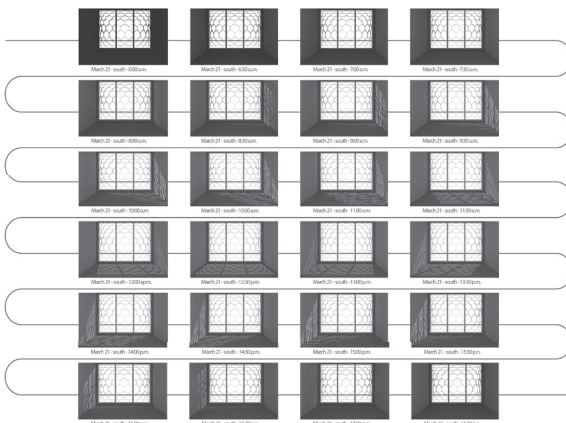


Figure 9. Interior shading analysis

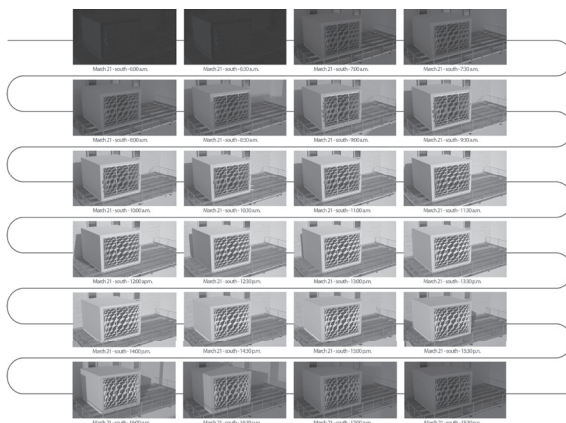


Figure 10. Exterior shading analysis

independent from the geometry of it's application, such as a building façade or roof plane. The majority of this work relied on preset modules in Grasshopper with slight modifications via VB script. The next step was to incorporate both the surface of application (building façade) and the pattern of articulation. The surface of application provided a base geometry on which to generate components. For our project, this was the thermal lab's south facing façade, but the model could accommodate a combination of surfaces, locations, and base geometries. Once the application surface was defined, we used phenomenological data as a basis for the component's patterning. For our purposes, exterior views at two station positions inside the lab and diffused light transmission provided a rudimentary data set though which a multiplicity of considerations could be tested. Patterning scenarios were judged by a number of quantifiable performance metrics.

The first metric was the ratio of obstructed view to shaded surface. In other words, questioning what is an acceptable amount of visual obstruction to shading ratio. Our final configuration was a 4% obstruction to 95% shading resulting in a 0.0421 impact—the closer the number is to zero, the lower the impact affecting the ratio. This ratio set drove our selection of grid configuration and building material. Based on our initial analysis of grid configurations, we developed an interlocking hexagonal grid, which allowed for greater structural stability than our initial rectilinear pattern. From this decision combined with the solar data, we designed an idealized shading structure specific to the thermal lab. To optimize this ideal configuration and to accommodate phenomenological data, we modified the hexagonal grid definition creating a plastic relationship between the two sets of information. By associating breadth of view and view corridors to void size, placement and shape, we were able to modify our base configuration into a more responsive configuration. We tested the flexibility of the configuration against desired view angles from two station points within the thermal lab (Figure 9 and 10). Component size was derived from a system of varying sized base surfaces, in which each shading component's geometric base was extracted. The desire to have views out was translated into larger voids giving way to smaller voids in a continuous morphological transformation between extremes. To control the range of morphological types, we amended the parametric model using a VB script to conform to a range of sizes based on the physical properties of our building material, in this case 1/8" polypropylene sheets. By varying the sizes of components that fit within a view

area, we were able to combine tightly packed components, which used the building material more efficiently with larger but less efficient components, allowing for better views. In either case, no component exceeded the span limits for our material, nor did any component become too small to use the joint types we designed.

The construction of the shading structure was also incorporated into our parametric model. In choosing to use polypropylene, we wanted a sheet material with good elastic properties, a relatively high strength to weight ratio, and a material that could be CNC milled. As we were developing our parametric model, we simultaneously tested the performance properties and manufacturing techniques for a number of possible materials. The variability of component sizes generated by our parametric model precluded many computer aided manufacturing techniques, which conclude that CNC milling was the only method that met our criteria.

Each component was created through an algorithmic process of subdividing, orienting, projecting, and cutting two-dimensional surfaces with three-dimensional entities. As such, our end component could be deconstructed into a single planar element, milled from a sheet of material and folded into form (Figure 11).

We automated this process, along with the joining system, to which there were three types (Figure 12 and 13):

- component to itself,
- component to component, and
- component array to thermal lab

Once the parametric model was complete, we could produce solution families and simulate their performance using Eco-tech as well as the output data from our own model. We looked at light quality, surface obstruction, view quality, and material usage to categorize the variety of tests (Figure 14). Based on these solutions, we chose a configuration to manufacture and compare volumetric and area dimensions to our initial analysis set (Figure 14)

Testing and Conclusions

After construction and installation, we began testing the shading structure and produced a comparative analysis with our initial conventional shading structures.

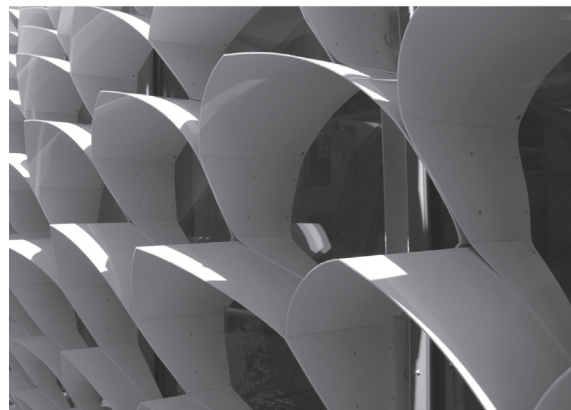
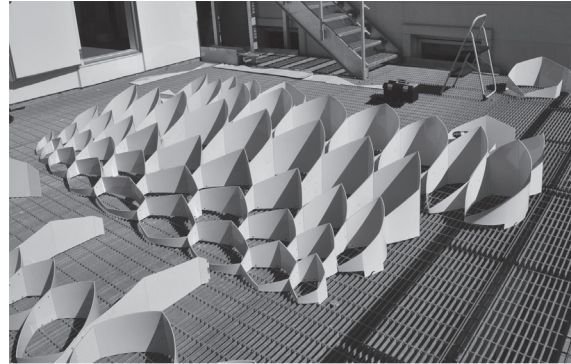


Figure 11. Unfolded component sample with embedded hanger system

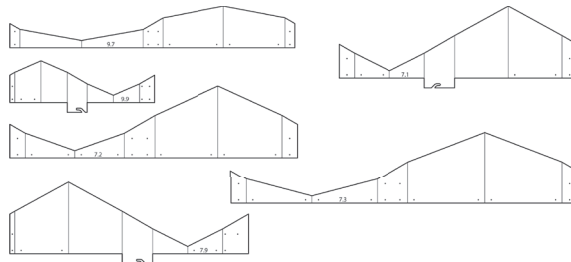


Figure 12. Shading structure detail in place on thermal lab



Figure 13. Exterior shading analysis



Figure 14. Exterior shading analysis
Figure 15. Shading structure in place on thermal lab

In addition to data collection on site, we produced a comparison of projected performance using Eco-tech. Based on our finding, two trends emerged. The shading structure provided almost complete shading (between 95%–100%) during our sample test period, a significant improvement over conventional shading configurations. However, overall thermal radiation increased over projected numbers for similar sized rectilinear grid configurations. This seeming discrepancy was actually a confirmation of an intended by-product of our configuration—diffused light transmission. Diffused light that contributed to solar radiation levels, but not heat gain had increased dramatically from our rectilinear grid simulation. Diffused light allows for better interior light quality, as well as a reduction in energy use from artificial light. This trend was most notable during sun positions

perpendicular to the greatest area of shading, typically high southern exposure (Figure 15). Second, shading to material efficiency was greatly increased (Figure 15). Because each component was optimized independently—based on its relationship to the sun and the façade—the amount of material used per area decreased significantly in comparison to conventional configurations. In addition, the interlocking hexagonal grid increased structural efficiency over orthogonal configurations.

The ability to incorporate both real world test results and simulated performances proved a difficult proposition. We reviewed data—not only dry numbers but associated those numbers with a multiplicity of effects. The use of site-specific input data allowed us to gain a control over how we formulate a response to design challenges. By contextualizing the solutions our model generated, we were able to think of design as a set of specific and control responses rather than as a singular solution. Information utilization requires a new way of crafting that moves beyond instances into relationships. For our shading structure, calibrating the relationships between input data and output form required careful design of both geometry and procedure.

Our goal is to continue evaluating the shading structure's performance over the summer season. We have begun analysis for a second test site—Munich, Germany—for the parametric model. With each iteration, we gain a better understanding of the architectural relationship between information and design. These relationships will prove to be transformative as architecture engages new technologies and as architects gain greater efficacy over how we impact our environment.

Acknowledgements:

The Responsive Shading project required expertise from multiple disciplines, without the hard work and guidance of the following faculty, staff, and students this project and its comprehensive approach would not have been possible. Thank you: Project Advising—Dr. Werner Lang, Technical University of Munich; Co-Advising—Dr. Atila Novoselac, Dason Whitsett, and Dr. Steven Moore, University of Texas, Austin; Digital manufacturing assistance—Paul Farmer, Eric Hepburn, and John Vehko, University of Texas, Austin; Data collection assistance—Hogan Winn; Renderings: Blake Smith and Stefan Bader.

Endnotes

(1) ASHRAE, 2009 ASHRAE Handbook - Fundamentals, <http://www.ashrae.org/publication>. 'Shading and fenestration attachments' 2009. This chapter provides the basic calculations needed for horizontal devices to be tilted in an ideal angle to provide maximum shading. This angle called the 'profile angle' or 'shadow-line angle' W can be calculated in relation to the solar altitude angle b as well as the solar azimuth angle g

$$\tan W = \tan b / \tan g$$

where W = profile or shadow-line angle

b = solar altitude angle

g = solar azimuth angle.